

# Fluorophore-Labeled Siloxane-Based Nanoparticles for Biomedical Applications

Olga Koshkina,<sup>1</sup> Christoph Bantz,<sup>2</sup> Christian Würth,<sup>1</sup> Thomas Lang,<sup>1</sup>  
Ute Resch-Genger,<sup>1</sup> Michael Maskos\*<sup>1</sup>

**Summary:** We present the synthesis and characterization of multifunctional fluorophore-labeled poly(organosiloxane) nanoparticles with core-shell architecture, where the fluorescent dye is incorporated into the core. Grafting of heterobifunctional poly(ethylene oxide) (PEO) onto the particle surface leads to water-soluble biocompatible nanoparticles. Two different strategies have been used for the synthesis: The encapsulation of dye-labeled monomers during the polycondensation with additional PEO coating and subsequent dye labeling by covalent attachment of the fluorescent dye rhodamine B to the (chloromethylphenyl)siloxane groups in the core after polymerization and grafting of PEO onto the surface. Comparison of the fluorescence quantum yields of the nanoparticles before and after PEO coating show a decrease in quantum yield after PEO coating.

**Keywords:** biocompatibility; core-shell; fluorescence; fluorescence quantum yield; nanoparticles; PEO

## Introduction

During the last decades, nanoparticles became objects of growing research interest, especially in biology and medicine, because of the wide range of applications they offer. One of the best investigated materials are silica nanoparticles due to the fact that they can be easily synthesized by the Stöber method.<sup>[1]</sup> The synthesis of fluorophore-labeled silica colloids via coupling of fluorescent dye molecules to the particle's surface and the formation of particles with core-shell structure, where the fluorescent dye is encapsulated in the core, have been previously reported.<sup>[2–6]</sup>

Aiming at biomedical applications, the surface properties become the most important factor for the interactions of nanoparticles with biological systems. As silica nanoparticles are electrostatically stabilized,

interactions between these colloids and oppositely charged biomolecules can lead to destabilization of the nanoparticles in biological media. Another challenge presents the subsequent surface modification of silica nanoparticles with e.g. targeting ligands and the formation of multi-compartment systems.

More flexible system are poly(organosiloxane) nanoparticles, due to their multi-compartment architecture and the possibility to introduce different reactive sites during the synthesis.<sup>[7–11]</sup> For example, the synthesis of amphiphilic nano networks and their dye loading have been previously reported as well as the synthesis of fluorophore-labeled siloxane nanospheres.<sup>[12–16]</sup> Both dye-loading and labeling were performed after the synthesis of the nanoparticles which can be also advantageous for the application of these poly-(organosiloxane) nanospheres as a potential drug carrier system. The functionalization of poly(organosiloxane) with PEO and subsequent coating of these particles with oligonucleotides and DNA led to water soluble, bio-functionalized nanoparticles.<sup>[17]</sup> Until present, however, the synth-

<sup>1</sup> BAM Federal Institute for Materials Research and Testing, Unter den Eichen 87, 12205 Berlin, Germany  
E-mail: Michael.Maskos@bam.de

<sup>2</sup> Institute of Physical Chemistry, University Mainz, Jakob-Welder-Weg 11, 55128 Mainz, Germany

esis of water-soluble poly(organosiloxane) nanoparticles efficiently labeled with fluorophores, which is essential for the tracing of these particles e.g. during cell experiments, could not be achieved.

## Experimental Part

### Materials

Water was purified with a Milli-Q deionizing system (Waters, Germany). All chemicals were used as received: trimethoxymethylsilane (T), diethoxydimethylsilane (D), dodecylbenzenesulfonic acid (DBA), triethoxysilane (T-H) (Wacker Chemie), (p-chloromethyl)phenyltrimethoxysilane (CIBz-T), 1,1,4,4-Tetramethyldisiloxane (M-H), Karstedt-Catalyst (ABCR, Germany), TWEEN 20, ethylene oxide (Fluka), rhodamine B, caesium iodide, 18-crown-6, toluene, methanol, dichloromethane, THF (Sigma-Aldrich). The dialysis tubing (regenerated cellulose; MWCO 10 kDa) was received from SpectrumLabs.

### Methods

For Asymmetrical Flow Field-Flow Fractionation (AF-FFF), an AF-FFF system 2.0 from Consensus, equipped with a Waters 486-UV detector (absorption measured at 254 nm) and a fluorescence detector F1110 from Merck-Hitachi (excitation at 540 nm, detection at 570 nm) was used. Polyether-sulfon membranes (MWCO 4000 g/mol) were utilized as semipermeable walls. Degassed Milli-Q water containing 5 mmol/L NaCl and TWEEN 20 was employed as eluent. Instrument calibration was performed with commercially available polystyrene latex standards (Duke, diameters 20, 50 and 100 nm).

Absorption spectra were measured with a Varian Cary 300 scan and fluorescence emission spectra with a Spex FL3-22 from Jobin Yvon Instruments S.A. using 1 cm-quartz cells.

The absolute fluorescence quantum yields ( $\Phi_f$ ) of the nanoparticles that equal the number of emitted photons ( $N_{em}$ ) per absorbed photons ( $N_{abs}$ ), were determined

at different stages of particle functionalization with a custom-designed integrating sphere setup. This setup consists of a xenon lamp coupled to a single monochromator and a six inch Spectrafect-coated integrating sphere (Labsphere GmbH) coupled with a quartz fiber to an imaging spectrograph (Shamrock 303i, Andor Inc.) with a Peltier cooled thinned back side illuminated deep depletion charge coupled device (CCD array) as detector. A reference detector was implemented into the setup to account for fluctuations of the radiant power reaching the sample. The spectral responsivity  $s(\lambda_{em})$  of the integrating sphere-detection system ensemble was determined with a calibrated quartz halogen lamp mounted inside an integrating sphere (Gigahertz-Optik GmbH).

For the measurement of the absolute fluorescence quantum yields  $\Phi_f$ , the sample or blank, i.e., the pure solvent in a conventional 1 cm-quartz cell was mounted into the center of the integrating sphere and the excitation light was focused into the middle of the cuvette. The absolute fluorescence quantum yield was calculated from the measured spectrally corrected signals of the blank ( $I_{CB}$ ) and the sample ( $I_{CS}$ ) in the wavelength region of the excitation ( $\lambda_{ex}$ ) and the emission ( $\lambda_{em}$ ) according to Equation 1.

$$\Phi_f = \frac{\int_{\lambda_{em1}}^{\lambda_{em2}} \frac{\lambda_{em}}{hc} (I_{CS}(\lambda_{em}) - I_{CB}(\lambda_{em})) d\lambda_{em}}{\int_{\lambda_{ex1}}^{\lambda_{ex2}} \frac{\lambda_{ex}}{hc} (I_{CB}(\lambda_{ex}) - I_{CS}(\lambda_{ex})) d\lambda_{ex}} = N_{em}/N_{abs} \quad (1)$$

$h$ : Planck constant;  $c$ : speed of light

As rhodamine B shows a considerable spectral overlap between absorption and emission (see Figure 3), the measured fluorescence quantum yields were corrected for reabsorption effects for high dye concentrations.<sup>[18]</sup>

### Synthesis

The caesium salt of rhodamine B (1 equivalent) and (p-chloromethyl)phenyl-tri-

methoxysilane (ClBz-T; 3 equivalents) were dissolved in THF. To increase the solubility, 18-crown-6 was added. The reaction mixture was stirred under argon at 55 °C for 48 hours. The solvent was evaporated and the residue resolved in dichloromethane, washed rapidly with water and dried over MgSO<sub>4</sub>. After evaporation of the solvent, a mixture of labeled monomer and ClBz-T was obtained. This mixture was used for particles synthesis without further purification.

The poly(organosiloxane) nanoparticles were synthesized in aqueous dispersion as described previously using 7 g T, 5 g D and 3 g ClBz-T for the core and 6 g T, 3 g D and 1 g T-H for the shell and DBA as surfactant. For the synthesis of dye-labeled particles, 1 g of ClBz-T was replaced by the dye-labeled monomer.<sup>[9,16,17]</sup>

The grafting of heterobifunctional PEO was performed as described before.<sup>[17]</sup>

For dye-labeling of PEO-coated nanoparticles, the particles were transferred into THF directly after the hydrosilation reaction using a rotary evaporator. Labeling was performed under the same conditions as the monomer synthesis. After evaporation of the solvent, the reaction mixture was resolved in water and purified by dialysis (MWCO 10 kDa).

## Results and Discussion

Poly(organosiloxane) core-shell nanoparticles with average radii of 10 nm were synthesized by condensation of different alkoxy silanes, including trimethoxymethylsilane (T), diethoxydimethylsilane (D), and (p-chloromethyl)phenyltrimethoxysilane (ClBz-T), in aqueous dispersion with dodecylbenzenesulfonic acid as surfactant and catalyst. Fluorophore-labeling of the core was achieved by incorporation of a rhodamine B-labeled monomer during the polycondensation.

The rhodamine B-labeled monomer (Figure 1) was synthesized by the substitution of the chlorine atom of (p-chloromethyl)phenyltrimethoxysilane (ClBz-T)

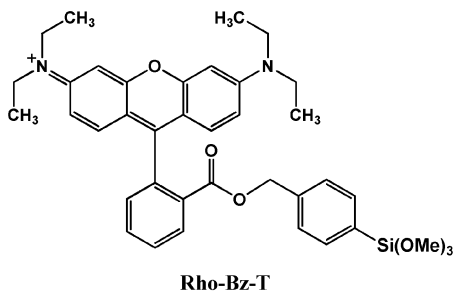


**Figure 1.**

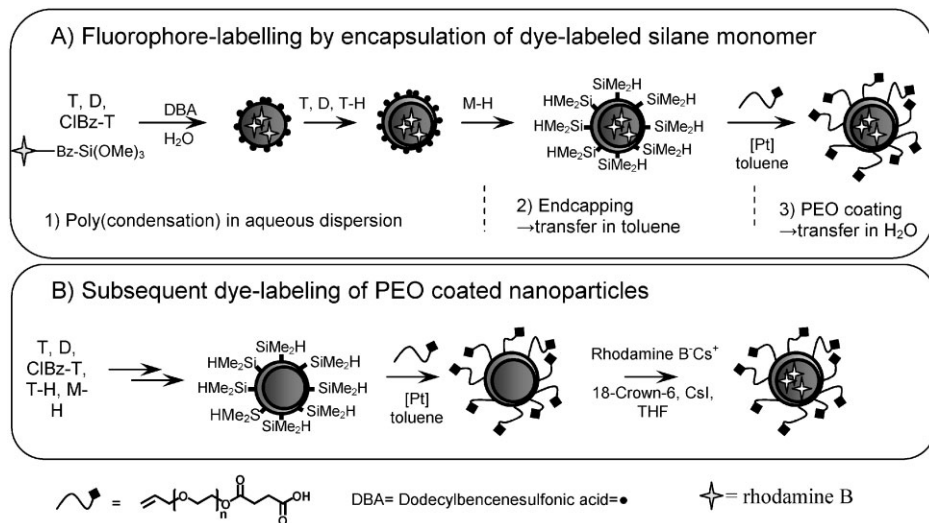
Dye-labeled monomer: rhodamine B-(p-trimethoxysilyl)benzylester.

by rhodamine B using the caesium salt of this dye. To improve the solubility of the dye-labeled monomer in the mixture of other monomers, an excess of ClBz-T was used for the reaction.

After the subsequent polycondensation of core and shell, silicon hydride functionalities were introduced into the particle's surface by endcapping with 1,1,4,4-tetra-methyldisiloxane (M-H). This surface functionalization provides solubility in organic solvents. No differences in the basic surface properties were observed compared to unlabeled particles.<sup>[10,11,19]</sup> As for the intended biomedical applications, water solubility is essential, heterobifunctional PEO was then grafted onto the surface in a hydrosilation reaction (Scheme 1, A).

Due to the network structure of the particles, fluorophore-labeling after PEO coating is another synthetic approach, which leads to water soluble rhodamine B-labeled nanoparticles (Scheme 1, B). This pathway allows the direct comparison of different functionalizations of otherwise identical nanoparticles by introduction of the corresponding functions, e.g. labeling with different fluorescent dyes, after the formation of the poly(organosiloxane) nanoparticles.

The sizes of the poly(organosiloxane) nanospheres were analyzed in the dry state by Transmission Electron Microscopy (TEM) and in solution by Asymmetrical Flow Field-Flow Fractionation (AF-FFF).<sup>[19]</sup> The radii of the dye labeled core-shell nanospheres are approximately



### Scheme 1.

Synthesis of fluorophore-labeled poly(organosiloxane) nanoparticles. A: Rhodamine B-labeling performed during the polycondensation by encapsulation of rhodamine B-labeled monomer. After subsequent endcapping with 1,1,4,4,-tetramethyldisiloxane and PEO-coating of the surface, rhodamine B-labeled, water-soluble particles were obtained. B: Subsequent fluorophore-labeling. After polycondensation and PEO-coating of unlabeled poly(organosiloxane) nanoparticles, the caesium salt of rhodamine B was covalently attached by the substitution of the chlorine atom of (p-chloromethyl)phenyltrimethoxysilane in the core of the nanoparticles.

9 nm (dry state) and the polydispersity is in the range of 20%. The AF-FFF measurements can also be used to demonstrate the success of the fluorophore-labeling reaction. As exemplified in Figure 2 for the aqueous dispersion of the nanoparticles, the nanoparticles can be detected with a

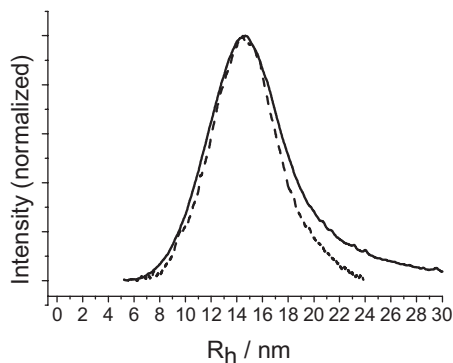


**Figure 2.**

AF-FFF fractogram of rhodamine B-labeled poly(organosiloxane) nanoparticles in aqueous dispersion. Dashed line: signal of UV detector; straight line: signal of fluorescence detector.

fluorescence detector during AF-FFF measurements.

The spectroscopic properties of the dye-labeled nanospheres were studied by fluorescence and absorption spectroscopy. The absorption and emission spectra of the free dye and the correspondingly labeled poly(organosiloxane) nanoparticles in toluene after endcapping are shown in Figure 3.

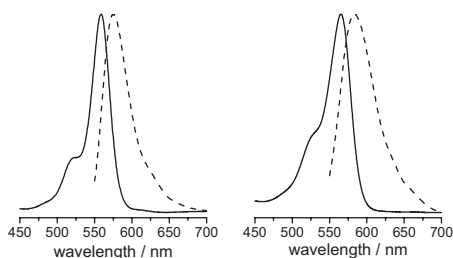


**Figure 3.**

Normalized absorption (black line) and emission (dashed line) spectra of the free dye monomer (solvent dichloromethane; left) and poly(organosiloxane) nanoparticles (solvent toluene; right), excitation was at 510 nm.

**Table 1.**

Absolute fluorescence quantum yields of rhodamine B-labeled poly(organosiloxane) nanospheres.

Sample (solvent)	Absolute fluorescence quantum yield
Rhodamine B-labeled monomer (solvent dichloromethane)	53%
Poly(organosiloxane) nanoparticles with encapsulated monomer after end-capping (solvent toluene)	46%
Poly(organosiloxane) nanoparticles with encapsulated monomer after PEO coating (solvent water)	10%
Poly(organosiloxane) nanoparticles, labeled after PEO coating (solvent water)	7%

These spectra reveal the characteristic features of rhodamine B.

In order to determine the influence of dye-labeling and subsequent surface functionalization on the fluorescence quantum yield of rhodamine B, we compared the absolute quantum yields of the free monomer and the absolute quantum yields of the rhodamine B-labeled nanoparticles. The results are summarized in Table 1.

The fluorescence quantum yield decreases only slightly during the encapsulation of the dye in the nanoparticles compared to the quantum yield of the free dye. Surface functionalization of the nanoparticles, i.e., PEO coating, however, leads to a considerable reduction in fluorescence. This effect can potentially be explained by a chemical modification of the dye by the platinum catalyst, which was used for PEO coating. Nevertheless, the fluorescence intensity of the PEO-modified nanoparticles is still high enough to enable the use of these materials for cell experiments.

## Conclusion

We have synthesized fluorophore-labeled poly(organosiloxane) nanoparticles by copolymerization of bi- and trifunctional siloxanes with a rhodamine B-labelled siloxane monomer. The core-shell architecture of these particles prevents the contact of the fluorescent dye with the (biological) environment. The introduction of silicon hydride reactive sites into the particle surface during the polymerization of the shell and the endcapping process allows subsequent modification of the

nanospheres by coating with heterobifunctional poly(ethylene oxide). This provides water solubility and biocompatibility of the synthesized nanoparticles and allows their further modification by conjugation of amino-functionalized biomolecules. In addition, to derive the influence of dye encapsulation and surface modification on the signal-relevant properties of these nanoparticles, the absolute fluorescence quantum yields of the monomer and the nanoparticles, synthesized via different synthetic routes were determined. Although PEO-coating leads to a decrease in quantum yield, the fluorescence intensity of the nanoparticles is still sufficient for cell experiments. To improve the fluorescence properties of these nanoparticles, alternative pathways of surface functionalization are currently being investigated.

**Acknowledgements:** We would like to thank Manfred Schmidt, Karl Fischer from Mainz University, and Ulrike Braun, Volker Wachten-dorf and Annabelle Bertin from BAM Federal Institute for Materials Research and Testing for fruitful discussions and DFG SPP 1313 as well as the German Ministry of Economics and Technology (BMWi; MNPQ-Vh 22-06) for financial support.

- [1] W. Stöber, A. Fink, E. Bohn, *Journal of Colloid and Interface Science* **1968**, 26, 62.
- [2] D. Kehrloesser, R.-P. Baumann, H.-C. Kim, N. Hampp, *Langmuir* **2011**, 27, 4149.
- [3] E. Herz, H. Ow, D. Bonner, A. Burns, U. Wiesner, *Journal of Materials Chemistry* **2009**, 19, 6341.
- [4] D. R. Larson, H. Ow, H. D. Vishwasrao, A. A. Heikal, U. Wiesner, W. W. Webb, *Chemistry of Materials* **2008**, 20, 2677.

- [5] N. A. M. Verhaegh, A. Van Blaaderen, *Langmuir* **1994**, 10, 1427.
- [6] A. Van Blaaderen, A. Vrij, *Langmuir* **1992**, 8, 2921.
- [7] F. Baumann, M. Schmidt, B. Deubzer, M. Geck, J. Dauth, *Macromolecules* **1994**, 27, 6102.
- [8] O. Emmerich, N. Hugenberg, M. Schmidt, S. S. Sheiko, F. Baumann, B. Deubzer, J. Weis, J. Ebenhoch, *Adv. Mater.* **1999**, 11, 1299.
- [9] C. Scherer, S. Utech, S. Scholz, S. Noskov, P. Kindervater, R. Graf, A. F. Thunemann, M. Maskos, *Polymer* **2010**, 51, 5432.
- [10] S. Utech, C. Scherer, K. Krohne, L. Carrella, E. Rentschler, T. Gasi, V. Ksenofontov, C. Felser, M. Maskos, *Journal of Magnetism and Magnetic Materials* **2010**, 322, 3519.
- [11] S. Utech, C. Scherer, M. Maskos, *Journal of Magnetism and Magnetic Materials* **2009**, 321, 1386.
- [12] C. Graf, W. Scharlt, K. Fischer, N. Hugenberg, M. Schmidt, *Langmuir* **1999**, 15, 6170.
- [13] C. Graf, W. Scharlt, M. Maskos, M. Schmidt, *Journal of Chemical Physics* **2000**, 112, 3031.
- [14] N. Jungmann, M. Schmidt, J. Ebenhoch, J. Weis, M. Maskos, *Angewandte Chemie-International Edition* **2003**, 42, 1714.
- [15] N. Jungmann, M. Schmidt, M. Maskos, *Macromolecules* **2003**, 36, 3974.
- [16] N. Jungmann, M. Schmidt, M. Maskos, J. Weis, J. Ebenhoch, *Macromolecules* **2002**, 35, 6851.
- [17] C. Diehl, S. Fluegel, K. Fischer, M. Maskos, *Surface and Interfacial Forces - from Fundamentals to Applications* **2008**, 134, 128.
- [18] C. G. Würth, M. Grabolle, J. Pauli, M. Spieles, U. Resch-Genger, *Analytical Chemistry* **2011**, 83, 3431.
- [19] C. Scherer, S. Noskov, S. Utech, C. Bantz, W. Mueller, K. Krohne, M. Maskos, *Journal of Nanoscience and Nanotechnology* **2010**, 10, 6834.